



Performance studies of Bifacial solar photovoltaic module installed at different orientations: Energy, Exergy, Enviroeconomic, and Exergo-Enviroeconomic analysis

Vimala Muthu¹ · Geetha Ramadas¹

Received: 2 September 2022 / Accepted: 7 March 2023 / Published online: 22 March 2023
© The Author(s), under exclusive licence to Springer-Verlag GmbH Germany, part of Springer Nature 2023

Abstract

One method for exploiting albedo-based power generation is the bifacial solar module (BFSM). It includes information on the bifacial solar module's energy, electrical and exergy efficiency, thermal exergy, and environmental analysis. The study contrasted the outcomes of the BFSM's east/west and north/south orientations. BFSM has been applied on both orientations with equal to latitude and equal to 30 degrees. The outcomes of all the aforementioned cases were compared and analyzed after outdoor experiments for the climatic condition were carried out in Minjur, Tamil Nadu. Under the specific climatic conditions, the 13-degree east/west module offers a shorter energy payback period, a better energy production factor (EPF), and a higher life cycle conversion efficiency (LCCE) when the life time of the system is considered as 10, 15, and 20 years. The environmental and economic analyses show that the most carbon credits from 13 degrees were earned with Rs. 14,925 and Rs. 192.89 from east/west module when the system's life was taken into account.

Keywords Bifacial solar · Exergy efficiency · Economic analysis · Life cycle conversion efficiency · Environmental analysis

Introduction

Thomas Alva Edison had suggested using solar energy before fossil fuels that vanished from the planet in 1931. At the moment, we are dependent on fossil fuels that contain carbon. The main reason to be concerned about the availability of energy in the future, however, is the elements of limited supply and growing pricing of all these sources. Utilizing sustainable energy sources, such as solar energy, which is accessible in India for about 300 light days per year, can help to a considerable part address these difficulties (Kandeal et al. 2020). The Suryamitra skill development program is a major initiative of the Honorable Prime Minister's "Make in India" initiative, by 2022, with a goal of 100 GW of solar power capacity.

According to modeled, measured, and simulated data, the average bifacial gains of an inclined south-facing stand-alone bifacial PV system over an inclined south-facing

stand-alone monofacial system is 10.15%, respectively. According to Yakubu et al. (2022), the slanted monofacial PV system performs better and generates more energy than the vertically mounted bifacial PV system at 0.25 albedo. Variable inclination angles are used for BFSM simulation and real-time testing. In this paper, the performance of the BFSM is examined using three simulation tools (MoBiDig, BIGEYE, and PVsyst). When the BFSM is positioned horizontally and vertically, there is reportedly a larger greatest deviation range of 10 W/m² between the measured and simulated sun intensities (Nussbaumer et al. 2020). Additionally, it is said that while the BFSM is pointed south, deviation is at its lowest level. With concentrated photovoltaic thermal (C-PVT) systems like the pure parabola (PP) and compound parabolic concentrator (CPC), the performance of a vertical BFSM is explored (Cabral and Karlsson 2018). A ray-tracing simulation tool is employed in this study to assess the system's thermal and electrical performance. According to reports, the BFSM coupled with the PP produces an annual yield of 267 Kwht/m² and 123 Kwhe/m². The annual yield of the BFSM integrated with the CPC is 309 Kwht/m² and 131 Kwhe/m², respectively. Experimental research was done to evaluate the BFSM's performance in the Qator desert (Baloch et al. 2020). In this study, authors conducted

Responsible Editor: Philippe Garrigues

✉ Vimala Muthu
mva.eee@rmkec.ac.in

¹ Department of Electrical & Electronics Engineering, R.M.K Engineering College, Kavaraipettai, Chennai 601206, India

BFSM optimization studies (changing mountain height, ground albedo, and panel temperature), as well as BFSM and MFSP comparative analyses. In comparison to putting the BFSM at a height of 66 cm, it was discovered that mounting it at a height of 103 cm generated the highest yield. Different materials (including grass, desert sand, aluminium, and white cement) are spread out on the ground in order to analyze the albedo differences. In comparison to the other tested materials, white cement spread out on the ground has provided a larger output. The greatest energy gain for a vertically mounted BFSM at 92-cm mounting height and a vertically installed BFSM with white cement on the ground, respectively, is around 28.5 and 22% when compared to the output of the MFSP. Additionally, it is stated that the BFSM installed vertically produces an average daily production of 5.28 Kwh whereas the MFSP only manages to create an average daily yield of 4.54 Kwh. In comparison to BFSM planted vertically, the BFSM installed at a 22° north–south angle performs better annually. Three crucial criteria for the construction of BFSM—inclination angle, height, and azimuth point—were optimized, according to a World Outlook article (Sun et al. 2018). Additionally, it is claimed that the height of the panel positioned above 1-m ground level increases the bifacial gain by 30%. If the panel angle is greater than 30, the BFSM's performance tends to degrade.

According to the modeling (optical–electrical–thermal) for BFSM that was developed (Gu et al. 2020), bifacial gain is larger during low-intensity periods due to more diffuse radiation. According to reports, BFSM mounting in an optimal inclination angle with tracking produces more than mounting in the east. In addition, it has been claimed that decreasing the BFSM inclination angle above latitude decreased the output of the panel relative to the panel positioned at the same latitude. In comparison to BFSM installed at an inclination angle above latitude, BFSM installed vertically provided a higher output.

According to research on the effects of temperature on BFSM and MFSP (Lamers et al. 2018), the temperature of the BFSM is 2 K lower than the MFSP. The BFSM performs better than the MFSP because its working temperature is lower than that of the MFSP's, which results in higher performance. In addition to comparing the temperatures of MFSP in two situations (glass–glass panel and back–sheet panel), researchers also looked at the temperatures of BFSM in three different ground environments (grassland, cement land, and water basin) (Zhang et al. 2020). It states that the BFSM's temperature is 54.7 °C, the MFSP's temperature with a back–sheet is 54 °C, and the MFSP's temperature with a glass–glass module is 55.7 °C. The BFSM's maximum temperature with cement land is 44.7 °C, whereas its maximum temperature 41.5 °C in water basin. Conferring to the given results, the BFSM's operating temperature is a little lower than the MFSP's. With 1-axis and dual-axis tracking

mechanisms, the comparative performance investigation of MFSP and BFSM is described (Rodri et al. 2020). According to published data, the energy yield of BFSM with 1-axis tracking is 35% higher than that of MFSP. (Lakshmi and Ramadas 2022) concluded that maximum efficiency loss of the solar PV module is found to be 73.51%, 66.29%, 65.46%, and 61.42%, respectively, for coal, sand, brick powder, and chalk dust; thus, coal dust is the most impacting dust sample among the four due to its maximum absorptivity and thus minimum transmissivity. It is also observed that the performance of the solar PV modules degraded when the temperature rose due to heat loss induced by dust accumulation.

According to economic research on MFSP and BFSM, the latter is more cost-effective when built above 40° latitudes than the former (Rodríguez-Gallegos et al. 2018). The authors conducted experimental research on the BFSM's interior performance in 3 situations, including BFSM with baffles, 3 modules, and open rack (Lopez-Garcia et al. 2019). The results of the experiments show that, when compared to the other two situations, the open rack setup produces the most power. Micro-facets were introduced by (Cook and Al-hallaj 2019) as a passive solar concentrator in BFSM for integration on windows. According to reports, the incorporation of micro-facets increased the panel's backside power generation by between 26.3 and 30.2%. Using PV panels, a building's architecture is created to reduce electrical energy usage (Yoo 2019). According to him, the proposed design produces 4% more power than a typical PV panel. Additionally, he claimed that adopting BFSM can enhance power output by 18%.

According to the intensity model developed for larger BFSM, these systems provided an energy output that was 20% higher than that of MFSPs (Durković and Đurišić 2019). Three different cases of vertical BFSM (flat cement ground, upward triangle, and downward triangle) were investigated (Khan et al. 2019). When erected at 40 and 60 degrees latitude, respectively, vertical BFSM under an upward triangle produces bifacial gains of 50 and 100 percent. Additionally, the outcomes demonstrate that a vertical BFSM installed at 40 N generated 30–50% more power than an equivalent MFSP. According to published research on the topic, BFSM should be tilted 10 to 15 degrees for locations above 30 degrees latitude (Patel et al. 2019). There have been published comparison studies on PV, PV/thermal (PV/T), BFSM, and BFSM thermal (BFSM/T) (Kuo et al. 2017). According to the findings, the BFSM/T system outperforms in terms of output and cost savings by 18% and 20%, respectively, than the PV/T system. Similar cost savings of 460% and a 210% increase in power output over PV output. However, compared to installing PV and PV/T, installing BFSM requires 11% more space.

In contrast, several researchers claimed that the MFSP temperature is higher than the BFSM (Li et al. 2011; F and Energy 2005; Maturi et al. 2014; Yusufoglu et al. 2015; King

et al. 2004). Yang et al. 2011; Guerrero-Lemus et al. 2016; Lamers et al. 2018; Appelbaum 2016; Li 2016; Ganiha 2017. Additionally, according to several authors' reports (de Wild-Scholten et al. 2007; Soria et al. 2015), both BFSM and MFSP have the same temperature (Molin et al. 2018). Researchers from diverse fields have examined the results of simulations on BFSM in several nations (Janssen et al. 2015; Berrian et al. 2019; Kuo et al. 2017; Yusufoglu et al. 2015; Shoukry et al. 2016; Chudinzow et al. 2019; Pelaez et al. 2019a, b). Less experimental work on the BFSM has been reported compared to simulation studies in countries like Saudi Arabia (Katsaounis et al. 2019), Germany (Shoukry et al. 2016), the USA (Pelaez et al. 2019a, b), Chile (Asgharzadeh et al. 2018; Stein et al. 2017), and South (Sugibuchi et al. 2013). Despite the numerous simulations and predictions that have been produced by different academics, according to the literature on BFSM research, however, there are not many experimental BFSM studies done in the weather of Tamil Nadu. As a result, the main objective of the current work is to research BFSM optimization in Minjur, Chennai, Tamil Nadu, India, given the local climate. Bifacial solar modules are more expensive than traditional monofacial solar modules, as they require more components and more advanced technology. However, they can generate more energy, which can offset the higher upfront cost. In addition, they require less space and less maintenance, which can also reduce the overall cost of a solar project. The findings of the proposed study will assist society and business in making the right decisions to adopt appropriate ground cover and enhance the performance of their solar module.

The following is how this paper is presented: Introduction is presented in "Introduction". Research gap is provided in "Research gap." Experimentation is covered in "Experimentation." Analysis part is explained in "Analysis." Result and discussion is presented in "Results and discussion." The manuscript's conclusion is presented in "Conclusion."

Research gap

The manuscript's primary objective is to investigate the scope of rooftop-mounted BFSM in the Minjur area in Tiruvallur District. The area of research need is to maximize the BFSM's orientation and inclination angle at the specifically chosen site. Although many studies have optimized monofacial solar modules in different parts of the world, this publication uses bifacial technology to analyze performance to get better results from the same amount of module coverage at a particular location. In order to move forward with the performance study of the bifacial modules, outside experiments (under natural sunlight) were first done on several orientations. The best angle of orientation is now to be selected.

Experimentation

Each of the two monocrystalline bifacial modules has a 416-Watt capacity, with the front and back power being 300 and 96 Watts, respectively. Table 1 contains the solar module's specifications.

For testing, the modules are connected to a 3.32-Ohm resistive DC load. On the rooftop, at a height of 11 m, the module is manually calibrated over 3600 times while utilizing iron. The frameless module is constructed with a rubber beading between the iron and module corners, and it weighs about 34 kg. In order to strengthen the base, it is best to tie the module to a paint bucket with cement packing and pebbles on top of concrete. Each module's four legs are organized in this uniform arrangement. The iron is painted once the structure has been set up to prevent rust from forming. According to Baloch et al. (2020), the module height is maintained at 100 cm from the ground clearance (Gu et al. 2020).

13.27° N and 80.26° E were the latitude and longitude of the experiment. The first module is designed to face eastward and westward, while the second module is pointed northward and southward. By altering the nuts and bolts at each position, the module was cambered. There are four different set-ups created, and they are as follows (Fig. 1):

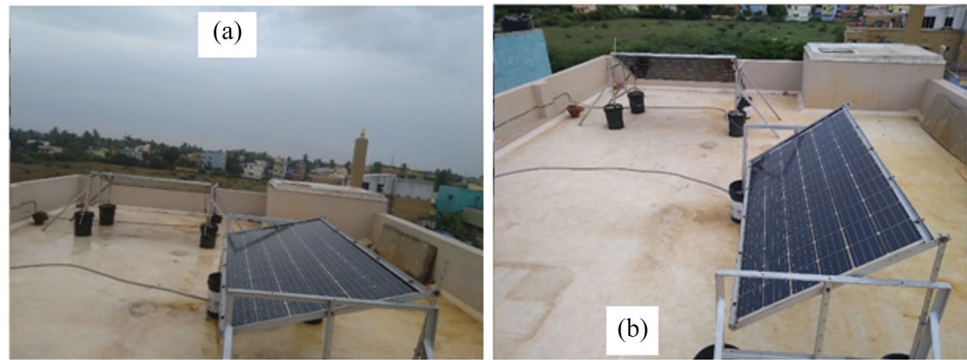
- Set A: north/south in an equal-latitude orientation against east/west
- Set B: north/south vs. east/west in a 30-degree orientation

In Chennai, the daily average temperature varies from 14 to 45 °C throughout the course of a year. The solar module was tested, and variables including ambient temperature, module temperature, wind speed, V_p , I_p and solar irradiation were recorded between the hours of 6 AM and 18 PM at one-hour intervals. The voltage and current are measured using a digital panel meter. An anemometer and a portable TES 132 solar power metre are used

Table 1 Module specifications

Model	Topsun	
Type	Monocrystalline	
Number of cells	72 cells	
	Front	Rear
Maximum voltage	37.20 V	37.20 V
Maximum current	8.61 A	2.58 A
Maximum power	320 W	96 W
Open circuit voltage	45.25 V	45.25 V
Short circuit current	9.10 A	2.73 A
Module efficiency	16.0%	4.8%

Fig. 1 Two bifacial modules are arranged experimentally in four distinct orientations for the suggested system. **a** Equal to latitude. **b** Equal to 30-degree orientation



to measure the wind speed and incident sun irradiation. Using a MECO digital multimeter, the temperature of the environment and the module is monitored.

Analysis

Energy efficiency

The PV module’s power output is determined by (Bayrak et al. 2017b)

$$P_{out} = V_{oc} * I_{sc} \tag{1}$$

where V_{oc} is the open circuit voltage, I_{sc} is the short circuit current, and FF is the fill factor. The fill factor is provided by

$$FF = \frac{V_p I_p}{V_{oc} I_{sc}} \tag{2}$$

where V_p is the voltage produced by the solar panel and I_p is the current drawn from the solar panel.

Energy efficiency is influenced by both the amount of solar energy that the PV module absorbs and the electrical power that it generates. Therefore, the ratio of electrical energy to the solar intensity received by the PV system, which is determined by the equation below, provides the maximum level of energy efficiency (Bayrak et al. 2017b).

$$\eta_{en} = \frac{V_{oc} I_{sc}}{S * A} \tag{3}$$

where S is the amount of solar energy that the PV module received.

Electrical efficiency

The relationship between the actual power output and the sun irradiation received by the surface area is known as electrical efficiency. (Joshi et al. 2009). Area is the area that the solar module covers (m^2).

$$\eta_{el} = \frac{V_p I_p}{S \times Area} \tag{4}$$

Electrical exergy

The system’s electrical exergy can be obtained from electrical energy and outside losses (Bayrak et al. 2017a).

$$E_{x_{elect}} = \text{Electrical energy} - \text{Electrical exergy destruction}$$

$$E_{x_{elect}} = V_p I_p \tag{5}$$

(or).

$$E_{x_{elect}} = V_{oc} I_{sc} FF \text{ (Joshi et al. 2009).}$$

Thermal exergy

The thermal exergy of the system is provided by heat loss from the PV surface, which comprises ambient and module temperature as well as heat released into the environment (Bayrak et al. 2017a).

$$E_{x_{therm}} = \left(1 - \frac{T_{amb}}{T_{module}} \right) Q \tag{6}$$

where T_{amb} is the temperature ambient in kelvin, T_{module} is the temperature of module in kelvin, Q is the heat released into the environment in Watts, h_{ca} is the heat transfer coefficient (W/m^2K), and u is the wind velocity (m/s).

$$Q = h_{ca} A (T_{panel} - T_{amb}) \tag{7}$$

$$h_{ca} = 5.7 + 3.8u \tag{8}$$

Exergy efficiency

The proportion of input to output energy is known as exergy efficiency.

The following provide input exergy:

$$E_{x_{in}} = \left(1 - \frac{T_{amb}}{T_{sun}}\right) AS_{max} \tag{9}$$

where T_{sun} is the temperature of clear sun which is considered as 5777 K and S_{max} is the solar radiation that the PV module has received.

Output exergy is as follows (Caliskan et al. 2012):

$$\eta_{x_{out}} = \frac{V_p I_p \left\{1 - \frac{T_{amb}}{T_{module}}\right\} h_{ca} A (T_{module} - T_{amb})}{\left(1 - \frac{T_{amb}}{T_{sun}}\right) AS_{max}} \tag{10}$$

Embodied energy

Calculating the amount of energy needed (or spent) over the whole life cycle of each material and product is the goal of embodied energy analysis is given in Table 2. Embodied energy provides an assessment of the total energy used to extract the raw materials and related components (Manokar et al. 2019).

Energy matrices

Energy matrices are the key element that provides a clear image of payback time in order to communicate about the viability of various renewable energy systems.

Three factors, including energy payback time, energy production factor, and life cycle conversion efficiency, can be used to analyze the system’s improved performance over its lifespan (Manokar, Ravishankar and Kabeel, 2019) (Shah-savar and Rajabi 2018).

Energy payback time (EPT)

EPT is the amount of time needed to complete all of the E_i involved in building the PV system, and it is defined as the proportion between the E_i (embodied energy) and E_o (annual obtained energy output) (Taylor et al. 2014).

$$\text{Energy Payback Time(EPT)} = \frac{E_i(\text{kWh})}{E_o(\text{kWh})}(\text{inyears}) \tag{11}$$

Energy production factor (EPF)

The factor used to assess the performance of the system under consideration is the energy production factor. EPF is calculated as the annual achieved energy production during the life time period (N) divided by the system’s embodied energy (Tripathi et al. 2017).

$$\text{Energy production factor (EPF)} = \frac{E_o \times N}{E_i} \tag{12}$$

Life cycle conversion efficiency (LCCE)

The difference between the yearly energy production for the system’s lifetime from the embodied energy and the annual solar irradiation energy (S_{annual}) received from the sun is what determines the LCCE efficiency. Life cycle efficiency is provided by (Tripathi et al. 2017)

$$\eta_{LCC} = \frac{(E_o \times N) - E_i}{S_{annual} \times N} \tag{13}$$

Exergoeconomic analysis

The exergoeconomic of an energy conversion system estimates and describes the cost of thermodynamic inefficiencies. This exergy-based approach acknowledges a relationship between exergy loss, capital expense, and time, leading to the achievement of a fully optimal design by appropriately balancing the exergy and economic characteristics. Equation can be used to compute the exergoeconomic parameter. (Tripathi and Tiwari 2019):

$$R_{exergo} = \frac{L_{ex,annualgain}}{UYC} \tag{14}$$

where $L_{ex,annualgain}$ is the annual overall exergy gain. UYC is the uniform end of annual cost:

Table 2 Embodied energy calculation

S. no	Materials	Embodied energy (kWh/kg)	Weight (kg)	Embodied energy (kWh)
1	PV module (kWh/m ²)	1130.56	2 (m ²)	2261.12
2	PV stand	7	10	70
3	Installation bucket	21.44	8	171.52
4	Cement	5.6	4	22.4
Total embodied energy (kWh)				2525.04

$$UYC = (P_c \times F_{CRF}) + M_c \times F_{CRF} - S_c \times F_{SRF} \tag{15}$$

P_c is the given by net present cost, which is the combination of the cost of PV modules and cost involved in the fabrication process; S_c is the salvage value, capital recovery factor is given by F_{CRF} ; M_c is the maintenance cost, F_{SRF} is the sinking fund factors, ROI is the rate of interest, and N is the number of years.

$$F_{CRF} = \frac{ROI \times (1 + ROI)^N}{(1 + ROI)^N - 1} \tag{16}$$

$$F_{SRF} = \frac{ROI}{(1 + ROI)^N - 1} \tag{17}$$

Enviroeconomic analysis

An average amount of 0.980 kgCO₂/kWh of CO₂ is released in a coal power plant (Tripathi and Tiwari 2019). Losses like distribution losses and transmission losses from the power plant to the consumer region as a result of improper electrical equipment and transmission systems. Therefore, it appears that 2.04 kg of CO₂ were released overall per kWh.

$$CO_2 \text{ annual mitigation in tonnes is } CO_2M = \frac{CO_2AE \times QEA}{1000} \tag{18}$$

where CO₂AE is the average CO₂ emissions from coal-based power generation (2.04 kg CO₂/kWh) and QEA is the overall thermal energy for the year.

CO₂ mitigation price per annum (enviroeconomic cost) is given by \$/year as (Zuhur and Ceylan 2019),

$$C_{CO_2M} = P_{cavg} \times CO_2M \tag{19}$$

Carbon price per tCO_{2e} is given by P_{cavg} (considering the average price as 14.5 \$/t CO₂).

Exergo-enviroeconomic analysis is the equivalent as enviroeconomic analysis, but exergy terms must be taken into account rather than energy words.

Analysis of experimental uncertainty

The uncertainty values of measuring instruments used experimentation are presented in Table 3.

An estimation of uncertainty is made for the experimental observations of different parameters. Experimental uncertainty is influenced by the measurement technique, observational process, environmental factors, calibration, and measurement error (error). Researchers examine the sample uncertainty analysis calculations for each set of readings by Agrawal and Rana (2019) and Tiwari et al. (1998). Equation (20) contains the uncertainty analysis' expression (22).

Table 3 Uncertainty of measuring instruments

S. no	Measuring device	Uncertainty (<i>U</i>)
1	Solar power meter–MECO Model 936	3.7%
2	K-type thermocouple	0.37%
3	MECO digital voltmeter	3.1%
4	MECO digital ammeter	2.94%

$$\% \text{ Uncertainty} = \frac{UCY}{AT} \times 100 \tag{20}$$

$$UCY = \sqrt{\frac{\sigma_1^2 + \sigma_2^2 \dots + \sigma_3^2}{T^2}} \tag{21}$$

$$\sigma = \sqrt{\frac{\sum (X - \bar{x})}{T_0}} \tag{22}$$

UCY stands for internal uncertainty; AT stands for average across all observations, for standard deviation across one set of observations; T stands for total number of observations; $(X - \bar{x})$ for deviation from mean, and T_0 stands for number of observations in one set. Solar irradiation, electrical efficiency, and power output have computed observations of uncertainty of 1.87%, 4.71%, and 2.53%, respectively.

Results and discussion

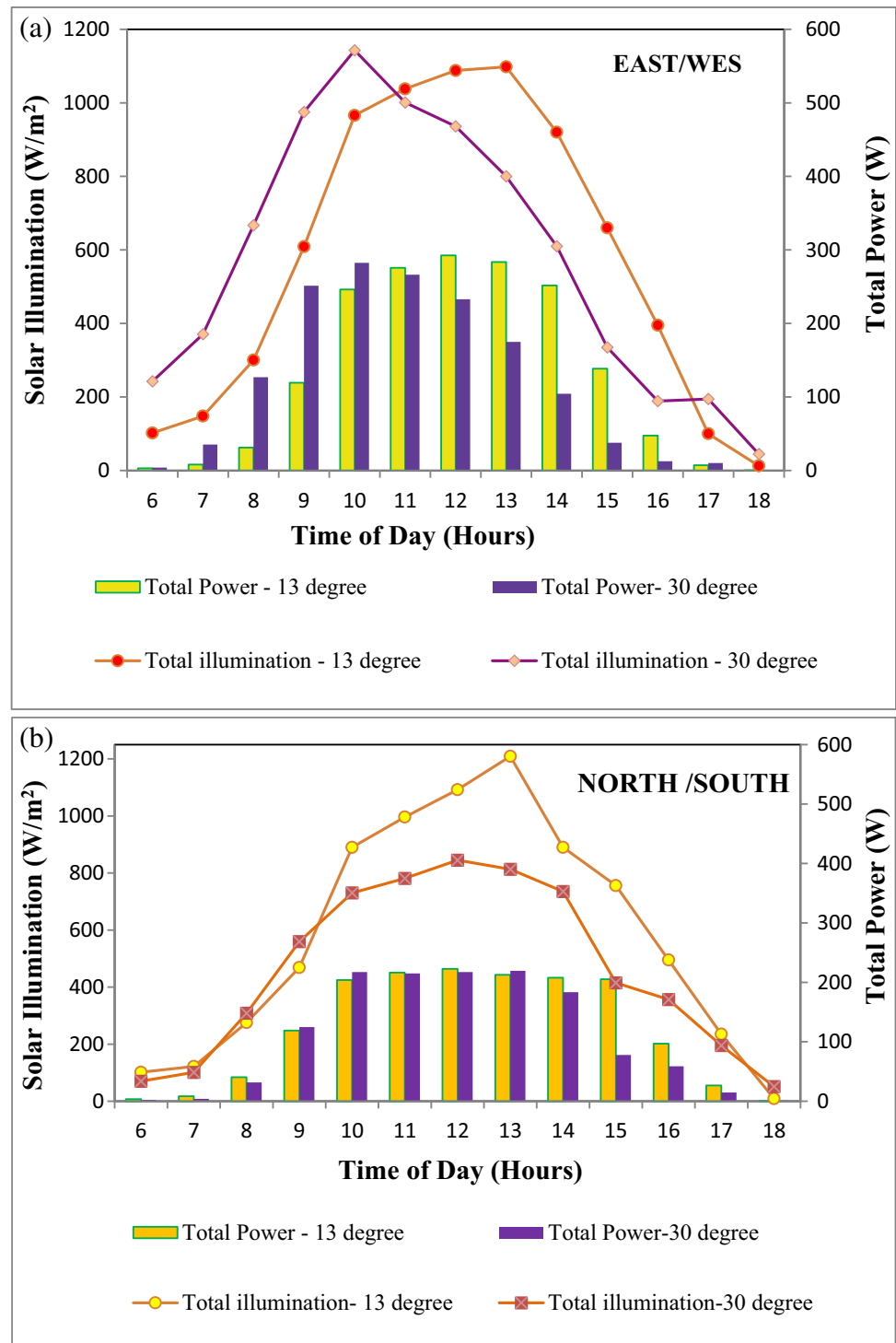
Daily variations in solar intensity

Figure 2a shows the daily variations in total solar intensity (front side + rear side) received by the BFSM at 13 degrees and 30 degrees of east/west orientation on 9.7.2020 and 21.7.2020, respectively.

On the equal to 13° inclined BFSM, the highest front side intensity and rear side intensity received are 795 and 233 W/m², respectively, in north/south directions. The BFSM may receive a maximum of 1098 W/m² of total solar intensity in an east/west direction and 1015 W/m² in a north/south direction. The diurnal average solar intensity collected on the front, back, and entire sides of the BFSM positioned in an east/west direction is 436.86 W/m², 135.23 W/m², and 572.1 W/m², respectively. In the same way, the values for north/south are 432.72, 147.21, and 579.9 W/m², respectively.

The 30° inclination BFSM receives the highest total solar intensity of 1143 W/m² in the east/west direction and 845 W/m² in the north/south direction. The diurnal average solar intensity collected on the front, back, and total

Fig. 2 **a** Total illumination and power output by BFSM vary on an hourly basis. **b** Total illumination and power produced by BFSM vary hourly



sides of the BFSM arranged in an east/west direction is 418.37 W/m², 159.16 W/m², and 577.5 W/m², respectively. In the same way, the values for north/south are 304.78, 153.69, and 458.5 W/m², respectively. It has been determined that BFSM facing east/west has gotten the highest solar intensity compared to BFSM facing north/south.

DC power produced from the BFSM at different orientations

The greatest DC power generated by the front side of the BFSM fixed on latitude of equal length and facing east/west is 268.3 W at 12:00 PM, the back side is 38.85 W at

1:00 PM, and the front and back sides combined generate 292.6 W at 12:00 PM. The BFSM's front, back, and combined front and back sides output an average daily DC power of 118.9, 12.22, and 131.1 W, respectively, when fixed at latitude of the same value and facing east/west. Similar to this, the highest DC power generated by the front side of the BFSM fixed on an equal latitude and facing north/south is 190.79 W at 12:00 PM, the back side of the BFSM is 34.45 W at 11:00 AM, and the front and back sides of the BFSM combined are 222.6 W at 12:00 PM. The BFSM's front side, back side, and combined front and back side output daily average DC power is 106.5, 13.76, and 120.3 W, respectively. The BFSM is fixed on an equal latitude and is orientated in a north/south direction.

The BFSM fixed at equal latitude and facing east/west produced 12.4 Watts more DC power at the front side of the BFSM fixed at equal latitude and north/south direction, according to a comparison analysis of the BFSM fixed at equal latitude and facing east/west and north/south directions. However, the BFSM's rear side facing east/west produced 1.54 W less DC power than the BFSM facing north/south. Due to the fact that the solar intensity receiving on the back side of the BFSM facing east/west is at a minimum (135.23 W/m^2) compared to the solar intensity receiving on the rear side of the BFSM facing north/south (147.21 W/m^2), this is the case. The total solar inputs obtained by the BFSM facing north/south were higher (579.9 W/m^2) than those received by the BFSM facing east/west (572.1 W/m^2). However, due to the BFSM operating temperature, DC power generated by the BFSM is at its highest when facing east/west. The highest BFSM was measured facing east/west at 56 degrees and facing north/south at 58 degrees. The average front and back sides of the BFSM were 41.1 and 41.38 degrees Celsius, respectively, while the front and back sides facing east/west were 42.77 and 42.46 degrees Celsius, respectively. It is evident from the thorough investigation that the BFSM's operating temperature affects DC power production significantly. The BFSM positioned on same latitude and facing east/west has produced greater output than the BFSM facing north/south from almost the same inputs conditions.

East/west and north/south modules with a tilt of 30 degrees each generate an average output of 118.4 W and 105.2 W, respectively. The largest result produced from the equal to latitude module was 131.1 W average, which was recorded by the east/west orientated 13 degree during the months of June and July when more illumination was seen due to the sun catastrophe.

Efficiency of the BFSM at different orientations

The performance of the BFSM installed at Minjur in June and July yields the efficiency shown in Figs. 3a and b. The

average efficiency of the east/west side oriented module tilted at an angle equal to latitude is 8.7%. The module displays an efficiency of 7.32% when tilted at a 30-degree angle.

Exergetic cost and uniform end of annual cost (UYC) of equal to 13 degree and equal to 30 degree for 15, 20, 25 and 25 years

Different combinations of the system's operating period—15, 20, 25, and 25 years—and interest rate are taken into consideration when calculating UYC and the related energetic cost of various facings (2%, 5%, and 10%). When the system's life is estimated to be 30 years with a 0.02% interest rate, the obtained values are given in Table 4. Higher change proficiency from the east/west module for all of the acquired orientations results in this.

Enviroeconomic and exergo-enviroeconomic analysis for different orientations

By using a PV system to generate electricity, carbon emissions can be significantly reduced, which helps combat climate change and mitigate the effects of global warming. Many countries and regions have environmental regulations that require companies to reduce their carbon footprint. By generating renewable electricity with a PV system, companies can earn carbon credits that can be used to offset their carbon emissions and comply with these regulations. Carbon credits have a monetary value and can be traded on carbon markets, creating a new revenue stream for companies that generate them. By focusing on the carbon credits that a PV system generates, companies can benefit financially from the system in addition to the energy savings it provides. By reducing carbon emissions, companies can enhance their corporate social responsibility and improve their reputation with customers, investors, and other stakeholders who are increasingly concerned about environmental sustainability. Focusing on the carbon credits of a PV system can help demonstrate a company's commitment to sustainability and environmental stewardship. The data on carbon mitigation and the credits obtained in terms of energy and exergy are provided by the reading from the exergo-enviroeconomic and enviroeconomic analyses, respectively. Table 4 shows that the equal to latitude–east/west module offers higher credits in terms of energy and that the equal to latitude–north/south module is higher in terms of exergy. LCCE of 0.169 is obtained from the 13-degree oriented east/west module and 30-degree installed north/south module.

Fig. 3 **a** Efficiency of the east/west oriented module varies hourly. **b** Efficiency hourly fluctuation from a north/south orientated module

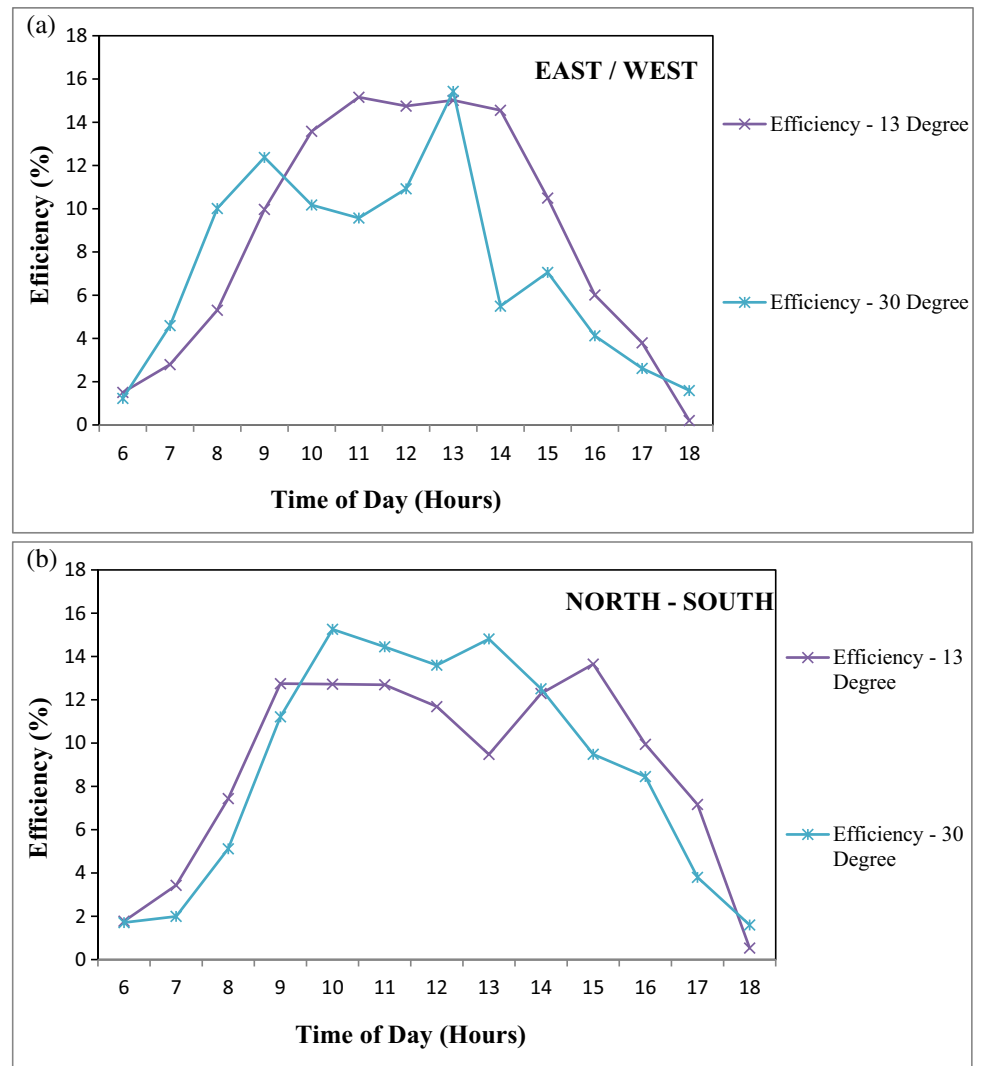


Table 4 Summary of analysis results

Parameter	East/west		North/south	
	13 degree	30 degree	13 degree	30 degree
Electrical efficiency	8.7	7.32	8.89	8.77
Exergy efficiency	7.91	7.47	7.93	8.62
Life cycle conversion efficiency	<i>N</i> = 10 years			
	0.169	0.151	0.144	0.169
	<i>N</i> = 15 years			
	0.183	0.165	0.158	0.186
Exergetic cost	<i>N</i> = 20 years			
	0.19	0.172	0.166	0.195
	<i>N</i> = 30 years & ROI=2%			
	0.16	0.15	0.14	0.13
$C_{CO_2M}(\text{energy})$	14,925	13,481.3	13,688.6	11,975.1
$C_{CO_2M}(\text{exergy})$	192.895	43.7048	464.678	22.4391

Conclusion

To determine the ideal orientation for the months of June and July for the particular site in Tamil Nadu, experiments were conducted. Therefore, four distinct tilt positions, including those equal to latitude and 30 degrees, are tested using the BFSM, with the last two positions tested using both the normal way of tilt and double the conventional tilt angle. Both east/west and north/south orientations are used to compare the two positions. The experimental results' conclusions are listed below, and the modules were made to deliver the DC load.

- i. The north/south orientated equal to latitude tilted module receives an illumination of 579.9 W/m² on average, which is the maximum. The second highest average illumination is received by a 577.5 W/m² East/West slanted module at a 30-degree angle.
- ii. When matching the mean power collected by the modules, it is found that equal-latitude tilted modules produce highest values of 120.3 W and 131.1 W, respectively, for both north/south and east/west oriented modules.
- iii. The average energy efficiency of modules oriented east/west is 7.91 percent and 7.47 percent, respectively. For modules oriented north/south, the average is 7.93% and 8.62%. Therefore, a module that is inclined 30 degrees from north to south offers improved energy efficiency.
- iv. The 13-degree east/west module provides 0.183 of the optimum LCCE when the system has a 15-year lifespan. Similarly, a module with a 30-degree north/south tilt offers 0.195 maximum LCCE over the course of the system's 20-year lifespan.

Future development will include integrating BFSM into building integrated systems, such as windows, roofs, and handrails, so that the PV system will become a part of the building and won't need to be installed somewhere else. Modern buildings are anticipated to include solar roofs that can be rendered transparent as needed.

Author contribution Conceptualization, methodology, resources, formal analysis, investigation, and writing—original draft preparation were carried out by Ms. M. Vimala. Review, editing, and supervision were carried out by Dr. Geetha Ramadas.

Data availability This is not applicable.

Declarations

Ethical approval This is not applicable.

Consent to participate This is not applicable.

Consent to publish This is not applicable.

Competing interests The authors declare no competing interest.

References

- Agrawal A, Rana RS (2019) Theoretical and experimental performance evaluation of single-slope single-basin solar still with multiple V-shaped floating wicks. *Heliyon* 5(4):e01525
- Appelbaum JJRE (2016) Bifacial photovoltaic panels field. *Renewable Energy* 85:338–343
- Asgharzadeh A, Marion B, Deline C, Hansen C, Stein JS, Toor F (2018) A sensitivity study of the impact of installation parameters and system configuration on the performance of bifacial PV arrays. *IEEE Journal of Photovoltaics* 8(3):798–805
- Baloch AAB et al (2020) In-field characterization of key performance parameters for bifacial photovoltaic installation in a desert climate. *Renew Energy* 159:50–63. <https://doi.org/10.1016/j.renene.2020.05.174>. (Elsevier Ltd)
- Bayrak F et al (2017a) A review on exergy analysis of solar electricity production. *Renew Sustain Energy Rev* 755–770. <https://doi.org/10.1016/j.rser.2017.03.012>. Elsevier Ltd, 74(June 2016)
- Bayrak F et al (2017b) A review on exergy analysis of solar electricity production a review on exergy analysis of solar electricity production. *Renew Sustain Energy Rev* 755–770. <https://doi.org/10.1016/j.rser.2017.03.012>. Elsevier Ltd, 74(July)
- Berrian D et al (2019) Performance of bifacial PV arrays with fixed tilt and horizontal single-axis tracking : comparison of simulated and measured data. *IEEE J Photovoltaics* IEEE 1–7. <https://doi.org/10.1109/JPHOTOV.2019.2924394>
- Cabral D, Karlsson BO (2018) Electrical and thermal performance evaluation of symmetric truncated C-PVT trough solar collectors with vertical bifacial receivers. *Solar Energy* 174(June):683–690. <https://doi.org/10.1016/j.solener.2018.09.045>. (Elsevier)
- Caliskan H, Dincer I, Hepbasli A (2012) A comparative study on energetic, exergetic and environmental performance assessments of novel M-Cycle based air coolers for buildings. *Energy Convers Manag* 56:69–79. <https://doi.org/10.1016/j.enconman.2011.11.007>. (Elsevier Ltd)
- Chudinzow D, Haas J, Díaz-Ferrán G, Moreno-Leiva S, Eltrop L (2019) Simulating the energy yield of a bifacial photovoltaic power plant. *Solar Energy* 183:812–822
- Lakshmi KR, Ramadas G (2022) Dust deposition's effect on solar photovoltaic module performance: an experimental study in India's tropical region. *J Renew Mater* 10(8):2133–2153
- Cook MJ, Al-hallaj S (2019) Film-based optical elements for passive solar concentration in a BIPV window application. *Solar Energy* 180(February 2018):226–242. <https://doi.org/10.1016/j.solener.2018.12.078>. (Elsevier)
- de Wild-Scholten MJ, Veltkamp AC, Energy ES (2007) Environmental life cycle analysis of dye sensitized solar devices; status and outlook. In 22nd European Photovoltaic Solar Energy Conference and Exhibition, pp 3-7
- Durković V, Đurišić Ž (2019) Extended model for irradiation suitable for large bifacial PV power plants. *Solar Energy* 191(August):272–290. <https://doi.org/10.1016/j.solener.2019.08.064>. (Elsevier)

- FAP, Energy R (2005) 07 Alternative energy sources (solar energy) 05 / 00237 Dimensioning , thermal analysis and experimental heat loss coefficients of an adsorptive solar icemaker 05 / 00241 Experimental determination of energy and exergy efficiency of the solar parabolic-c. (January), p 2005
- Ganilha SC (2017) Potential of bifacial PV installation and its integration with storage solutions. (Doctoral dissertation)
- Gu W et al (2020) A coupled optical-electrical-thermal model of the bifacial photovoltaic module. *Appl Energy* 258(August 2019):114075. <https://doi.org/10.1016/j.apenergy.2019.114075>. (Elsevier)
- Guerrero-lemus R et al (2016) Bifacial solar photovoltaics – a technology review'. *Renew Sustain Energy Rev* 60:1533–1549. <https://doi.org/10.1016/j.rser.2016.03.041>. (Elsevier)
- Janssen GJM et al (2015) Outdoor performance of bifacial modules by measurements and modelling. *Energy Proc* 77:364–373. <https://doi.org/10.1016/j.egypro.2015.07.051>. (Elsevier B.V)
- Joshi AS, Dincer I, Reddy BV (2009) Thermodynamic assessment of photovoltaic systems. *Solar Energy* 83(8):1139–1149. <https://doi.org/10.1016/j.solener.2009.01.011>. (Elsevier Ltd)
- Kandael AW et al (2020) Photovoltaics performance improvement using different cooling methodologies: a state-of-art review. *J Clean Prod.* 273:122772. <https://doi.org/10.1016/j.jclepro.2020.122772>. (Elsevier Ltd)
- Katsaounis T et al (2019) Performance assessment of bifacial c-Si PV modules through device simulations and outdoor measurements. *Renewable Energy* 143:1285–1298. <https://doi.org/10.1016/j.renene.2019.05.057>. (Elsevier Ltd)
- Khan MR et al (2019) Ground sculpting to enhance energy yield of vertical bifacial solar farms. *Applied Energy* 241(March):592–598. <https://doi.org/10.1016/j.apenergy.2019.01.168>. (Elsevier)
- King DL, Boyson WE, Kratochvill JA (2004) Photovoltaic array performance model. (December) Photovoltaic array performance model, United States. Department of Energy 8:1–19
- Kuo CW, Kuan TM, Wu LG, Huang CC, Peng SI, Yu CY (2017) Optimized back side process for high performance mono silicon PERC solar cells. In 2016 IEEE 43rd Photovoltaic Specialists Conference (PVSC) IEEE, New York, pp 2928–2930
- Lamers MWPE et al (2018) Solar energy materials and solar cells temperature effects of bifacial modules : hotter or cooler ? 185(May):192–197. <https://doi.org/10.1016/j.solmat.2018.05.033>
- Li B et al (2011) Simulation and testing of cell operating temperature in structured single and double glass modules. In 2011 37th IEEE Photovoltaic Specialists Conference. IEEE, New York, pp 003189–003194
- Li CT (2016) Development of field scenario ray tracing software for the analysis of bifacial photovoltaic solar panel performance (Doctoral dissertation, Université d'Ottawa/University of Ottawa)
- Lopez-Garcia J, Casado A, Sample T (2019) Electrical performance of bifacial silicon PV modules under different indoor mounting configurations affecting the rear reflected irradiance. 177(July 2018):471–482. <https://doi.org/10.1016/j.solener.2018.11.051>
- Manokar AM, Ravishankar MV, Kabeel AE (2019) Enhancement of potable water production from an inclined photovoltaic panel absorber solar still by integrating with flat - plate collector. *Environment, Development and Sustainability*. Springer Netherlands. (0123456789). <https://doi.org/10.1007/s10668-019-00376-7>
- Maturi L et al (2014) BiPV system performance and efficiency drops : overview on PV module temperature conditions of different module types. *Energy Proc.* 48:1311–1319. <https://doi.org/10.1016/j.egypro.2014.02.148>. (Elsevier B.V)
- Molin E et al (2018) Experimental yield study of bifacial PV modules in Nordic conditions. *IEEE Journal of Photovoltaics* 8(6):1457–1463
- Nussbaumer H et al (2020) Accuracy of simulated data for bifacial systems with varying tilt angles and share of diffuse radiation. *Solar Energy* 197(December 2019):6–21. <https://doi.org/10.1016/j.solener.2019.12.071>. (Elsevier)
- Patel MT et al (2019) A worldwide cost-based design and optimization of tilted bifacial solar farms. *Appl Energy* 247(March):467–479. <https://doi.org/10.1016/j.apenergy.2019.03.150>. (Elsevier)
- Pelaez SA, Deline C, Macalpine SM et al (2019a) Comparison of bifacial solar irradiance model predictions with field validation. *IEEE Journal of Photovoltaics* 9(1):82–88
- Pelaez SA, Deline C, Greenberg P et al (2019b) Model and validation of single-axis tracking with bifacial PV. *IEEE Journal of Photovoltaics*. IEEE pp. 1–7. <https://doi.org/10.1109/JPHOTOV.2019.2892872>
- Rodríguez-Gallegos CD et al (2018) Monofacial vs bifacial Si-based PV modules: which one is more cost-effective ? *Solar Energy* 176(August):412–438. <https://doi.org/10.1016/j.solener.2018.10.012>. (Elsevier)
- Rodri CD et al (2020) Article global techno-economic performance of bifacial and tracking photovoltaic systems global techno-economic performance of bifacial and tracking photovoltaic systems. pp. 1–28. <https://doi.org/10.1016/j.joule.2020.05.005>
- Shahsavari A, Rajabi Y (2018) Exergoeconomic and enviroeconomic study of an air based building integrated photovoltaic / thermal (BIPV / T) system. *Energy* 144:877–886. <https://doi.org/10.1016/j.energy.2017.12.056>. (Elsevier Ltd)
- Shoukry I et al (2016) Modelling of bifacial gain for stand-alone and in-field installed bifacial PV modules. *Energy Proc* 92:600–608. <https://doi.org/10.1016/j.egypro.2016.07.025>. (The Author(s))
- Soria B et al (2015) A study of the annual performance of bifacial photovoltaic modules in the case of vertical facade integration. *Res Article*. <https://doi.org/10.1002/ese3.103>
- Stein JS, Burnham L, Lave M (2017) One year performance results for the prism solar installation at the New Mexico Regional test center : field data from February 15 , 2016 - February 14 , 2017. (June)
- Sun X, Khan MR, Deline C, Alam MA (2018) Optimization and performance of bifacial solar modules: a global perspective. *Appl Energy* 212:1601–1610. <https://doi.org/10.1016/j.apenergy.2017.12.041>
- Sugibuchi K, Ishikawa N, Obara S (2013) Bifacial-PV power output gain in the field test using “EarthON” High bifaciality solar cells. 28th European photovoltaic solar energy conference and exhibition. <https://doi.org/10.4229/28thepvsec2013-5bv.7.72>
- Taylor P, Sudhakar K, Srivastava T (2014) Energy and exergy analysis of 36 W solar photovoltaic module. *Int J Ambient Energy* (September) 37–41. <https://doi.org/10.1080/01430750.2013.770799>
- Tripathi R, Tiwari GN (2019) Energy matrices, life cycle cost, carbon mitigation and credits of open-loop N concentrated photovoltaic thermal (CPVT) collector at cold climate in India : a comparative study. *Solar Energy* 186(May):347–359. <https://doi.org/10.1016/j.solener.2019.05.023>. (Elsevier)
- Tripathi R, Tiwari GN, Dwivedi VK (2017) Energy matrices evaluation and exergoeconomic analysis of series connected N partially covered (glass to glass PV module) concentrated- photovoltaic thermal collector : at constant flow rate mode. *Energy Convers Manag* 145:353–370. <https://doi.org/10.1016/j.enconman.2017.05.012>. (Elsevier Ltd)
- Tiwari GN, Khan ME, Goyal RK (1998) Experimental study of evaporation in distillation. *Desalination* 115(2):121–128
- Yakubu RO, Ankoh MT, Mensah LD, Quansah DA, Adaramola MS (2022) Predicting the potential energy yield of bifacial solar PV systems in low-latitude region. *Energies* 15(22):8510
- Yang L et al (2011) High efficiency screen printed bifacial solar cells on monocrystalline CZ silicon. July 2010. pp. 275–279. <https://doi.org/10.1002/pip>

- Yoo S (2019) Optimization of a BIPV system to mitigate greenhouse gas and indoor environment. *Solar Energy* 188(May):875–882. <https://doi.org/10.1016/j.solener.2019.06.055>. (Elsevier)
- Yusufoglu UA, Pletzer TM, Koduvelikulathu LJ (2015) Analysis of the annual performance of bifacial modules and optimization methods. *IEEE Journal of Photovoltaics* 5(1):320–328
- Zhang Z et al (2020) The mathematical and experimental analysis on the steady-state operating temperature of bifacial photovoltaic modules. *Renew Energy* 155:658–668. <https://doi.org/10.1016/j.renene.2020.03.121>. (Elsevier Ltd)
- Zuhur S, Ceylan İ (2019) Energy, exergy and enviroeconomic (3E) analysis of concentrated PV and thermal system in the winter

application. *Energy Rep* 5:262–270. <https://doi.org/10.1016/j.egy.2019.02.003>

Publisher's note Springer Nature remains neutral with regard to jurisdictional claims in published maps and institutional affiliations.

Springer Nature or its licensor (e.g. a society or other partner) holds exclusive rights to this article under a publishing agreement with the author(s) or other rightsholder(s); author self-archiving of the accepted manuscript version of this article is solely governed by the terms of such publishing agreement and applicable law.